Regulated Cl Transport, K and Cl Permeability, and Exocytosis in T84 Cells

Margaret E. Huflejt, Ronald A. Blum, Steven G. Miller, Hsiao-Ping H. Moore, and Terry E. Machen
Division of Cell and Developmental Biology, Department of Molecular and Cell Biology, University of California, Berkeley, California 94720

Abstract

We measured stimulant-induced changes of exocytosis that are associated with increases in Cl secretion (i.e., short circuit current, I_{SC}, in $\mu A/cm^2$) and apical (ap) Cl permeability (P_{Cl}) and basolateral (bl) K permeability (P_K) (both in cm/s) in T84 monolayers. P_{Cl} and P_K were measured by permeabilizing the bl or ap membrane with nystatin. P_{Cl} was also measured with a fluorescent dye 6-methoxy-*N*-(3-sulfopropyl)quinolinium (SPQ). A noninvasive and sensitive method (release of $^{35}SO_4$-labeled glycosaminoglycan [GAG], a fluid-phase marker of Golgi-derived vesicles) was used to measure exocytosis at both ap and bl membranes. At rest, $I_{SC} = 3.6$, $P_K = 0.8 \times 10^{-6}$, $P_{Cl} = 2.1 \times 10^{-6}$ with SPQ and 2.4×10^{-6} electrically, and there was constitutive GAG secretion (i.e., exocytosis) to both ap and bl sides (bl >2 × ap). Carbachol (C) increased: I_{SC} ($\Delta = 18.6$), P_K (6.5×), P_{Cl} (1.8–2.9×), and exocytosis to both ap (2.2–3.5×) and bl (2.0–3.0×) membranes. Forskolin (F) increased I_{SC} ($\Delta = 29$), P_{Cl} (5.5–11×) and ap exocytosis (1.5–2×), but had no effect on P_K or bl exocytosis. Synergistic effects on I_{SC} occurred when C was added to F-treated cells but not vice versa, even though the characteristic effects of F + C on P_{Cl}, P_K, and/or GAG secretion were identical to those exhibited when stimulants were added individually. Cl secretion results from coordinated activation of channels at ap and bl membranes, and exocytosis may play a role in these events. (*J. Clin. Invest.* 1994. 93:1900–1910.) Key words: Cl secretion • carbachol • forskolin • nystatin • Golgi vesicles • 4-methylumbelliferyl-β-D-xyloside

Introduction

Cl secretion by monolayers of (human colonic adenocarcinoma), T84 epithelial cells results from the coupling of four ion transport processes. $Na/K/Cl_2$ cotransport, K channels, and Na/K-ATPase are located at the basolateral membrane and facilitate Cl entry and Na and K recycling; Cl then exits the cell via apical Cl channels down its electrochemical gradient (1–3). Increases in Cl secretion may occur by activating the pumps and channels that are already present in the membrane and/or by fusing (exocytosis) intracellular vesicles that contain channels and transporters with the plasma membrane. Previous work has concentrated on exocytotic events that occur at the apical membrane. For example, in gastric parietal cells (4), turtle bladder cells (5), and renal intercalated cells (6), cellular activation by secretagogues leads to the fusion of cytoplasmic vesicles containing H pumps and Cl channels. H, Cl, and water transport persists until the stimulant is removed, at which time the pumps and channels are endocytosed and recycled (7). Other examples of exocytotic activation include the following: endosomes from kidney proximal tubules have cAMP-dependent Cl conductance which likely represent plasma membrane channels that have been endocytosed (8); Ca-transporting cells from distal renal tubules insert Ca channels into the apical membrane during parathyroid hormone stimulation in a microtubule-dependent exocytosis (9); and water channels of kidney epithelial cells are inserted and recycled at the apical membrane under the control of vasopressin (8). Stimulant-controlled vesicular traffic may also occur at the basolateral side of epithelial cells. Carbachol induces recycling of Na/K-ATPase from intracellular vesicles to basolateral membranes of rat lacrimal cells (10, 11), and H/HCO_3 transport at the basolateral membrane of pancreatic duct cells may also be regulated by exocytotic fusion (12).

There has recently been a surge of interest in the roles of exocytosis and endocytosis in controlling Cl permeability in epithelia that contain the cystic fibrosis transmembrane conductance regulator (CFTR),[1] and the results have been controversial. Activation of T84 cells with cAMP caused increases in exocytosis (13, 14) and decreases in endocytosis (14, 15). These processes were both defective in cells derived from a CF patient (CFPAC), and the defects were reversed by transfection with the complementary DNA encoding the wild-type CFTR gene (13). These studies of exocytosis and endocytosis did not utilize polarized cells, so it was not possible to determine whether the events were occurring at the apical or basolateral membrane. Antibody labeling of the CFTR (15, 16) has shown that the CFTR was constitutively expressed on the apical membrane of T84 cells, and this expression did not increase during forskolin stimulation, as would be expected if there had been an exocytotic delivery of CFTR to the apical membrane (16). These antibody labeling experiments may not have been sensitive enough to measure relatively small differences in exocytoic delivery of CFTR to the membrane.

In order to determine whether exocytosis of Golgi-derived membrane vesicles may play a role in the activation of both

Dr. Huflejt's present address is Department of Psychiatry and Langley Porter Psychiatric Institute, University of California, San Francisco, CA 94143-0984; Dr. Miller's present address is Parnassus Pharmaceuticals, Inc., 1501 Harbor Bay Parkway, Alameda, CA 94501.

Address correspondence to Dr. Terry Machen, Division of Cell and Developmental Biology, Department of Molecular and Cell Biology, 231 Life Sciences Addition, University of California, Berkeley, CA 94720.

Received for publication 19 July 1993 and in revised form 21 December 1993.

J. Clin. Invest.

0021-9738/94/05/1900/11 $2.00
Volume 93, May 1994, 1900–1910

1. *Abbreviations used in this paper:* CFTR, cystic fibrosis transmembrane conductance regulator; GAG, glycosaminoglycan(s); SPQ, 6-methoxy-*N*-(3-sulfopropyl)quinolinium; xyloside, 4-methylbelliferyl-β-D-xyloside.

apical Cl and basolateral K channels in polarized T84 monolayers, we measured the time courses of the forskolin and/or carbachol-induced activation of Cl secretion, apical Cl permeability (P_{Cl}), basal K permeability (P_K), and the polarized exocytosis of Golgi-derived vesicles. Transepithelial short-circuit current (I_{SC}) was used to quantitate net active Cl transport (17). We measured both basolateral P_K and apical P_{Cl} in nystatin-permeabilized T84 monolayers using electrophysiological methods. Apical P_{Cl} was confirmed using a fluorescent Cl indicator to monitor intracellular [Cl]. A noninvasive, reliable, and sensitive assay of exocytosis based on quantitation of $^{35}SO_4$-labeled glycosaminoglycans as fluid-phase markers of Golgi-derived vesicles (see reference 18) was used to determine the time course and magnitude of fusion of Golgi-derived vesicles with the apical and basolateral membranes.

Methods

Chemicals and solutions

All chemicals were reagent grade and, unless otherwise specified, obtained from Sigma Chemical Co. (St. Louis, MO). Stock solutions of 0.5 M 4-methylumbelliferyl-β-D-xyloside (xyloside), 10 mM forskolin (Calbiochem Corp., La Jolla, CA), 10 mM nigericin, 10 mM triphenyl-*N*-tin, and 4.4 mg/ml nystatin were prepared in DMSO and stored at −20°C. Stock solutions of 100 mM carbamylcholine (carbachol) and 5 mM ouabain were prepared in double distilled H_2O and stored at 4°C. The fluorescent chloride indicator 6-methoxy-*N*-(3-sulfopropyl)quinolinium (SPQ) was purchased from Molecular Probes Inc. (Eugene, OR). DME H-16/F-12 (1:1) and penicillin-streptomycin (100×) were obtained from the Cell Culture Facility (University of California, San Francisco). Newborn calf serum was obtained from Gemini Bioproducts (Calabasas, CA).

The following solutions (listed in Table I) were used in the experiments to determine I_{SC}, P_{Cl}, and P_K in Ussing chambers: (1) NaCl Ringer's; (2) $NaNO_3$; (3) high K/low Na/gluconate; (4) low K/low Na/gluconate; (5) high Cl/high K; and (6) low Cl/high K. Solutions were aerated, buffered to pH 7.4 and maintained at 37°C during the course of the experiments. Final concentration of secretory agonists was 10 μM for forskolin and 100 μM for carbachol.

Table I. Solutions

Component	Solution 1	2	3	4	5	6
NaCl	140				10	
Na gluconate			10	10		10
NMG-gluconate				135		
KCl	5				140	
K gluconate			140	5		140
$CaCl_2$	1				1	
$MgCl_2$	1					
$MgSO_4$		1	1	1	1	1
$NaNO_3$		135				
KH_2PO_4		0.6				
$K_2HPO_43H_2O$		2.4				
Ca gluconate			1	1		1
$CaSO_4$		1				

Composition of solutions used for permeability determinations. All concentrations are given in mM/liter. All solutions also contained 10 mM glucose and 10 mM Hepes and were pH 7.4.
Abbreviation: NMG, *N*-methyl-D-glucamine.

Cell culture. T84 cells (passages 50–62) were grown (17) either on permeable polycarbonate filters (3.0-μm pore size, 24-mm diam, Costar Inc., Cambridge, MA) for measurements of I_{SC}, P_K, P_{Cl}, and exocytosis, or on glass coverslips for Cl microspectroflourimetry (seeding density of 2.5×10^5 cells/cm^2) in a humidified atmosphere of 95% air and 5% CO_2 at 37°C. Both polycarbonate membranes and glass coverslips were precoated with human placental collagen (100 μg/ml). The cells were grown in DME H-16/F-12 (1:1) containing 5% newborn calf serum, penicillin (100 U/ml), streptomycin (100 μg/ml), 15 mM Hepes, 17.5 mM glucose, and 2.5 mM glutamine. The growth medium was changed every 2–3 d; 5–8-d-old monolayers with transepithelial resistance (R_T) > 800Ω × cm^2 (as measured by EVOM "chopstick" electrodes, World Precision Instruments, Inc., New Haven, CT) were used in experiments in which current, permeabilities, or exocytosis were measured.

Short circuit current measurements. Filters on which cells had grown to confluency were fitted into a plastic adapter ring and mounted into an Ussing chamber (17) with NaCl Ringer's on both sides of the monolayer. Short-circuit current (I_{SC}) was measured using a standard four electrode voltage clamp (710E-1 University of Iowa). All I_{SC} measurements were recorded on a chart recorder as well as on an IBM compatible computer through an analog/digital board (DataQ Instruments, Akron, OH).

Cl secretion was measured (as the I_{SC}) with NaCl Ringer's (solution 1, Table I) on both sides of the epithelial monolayer.

Basolateral K conductance was measured by permeabilizing the apical membrane to all small monovalent ions with nystatin (19) and then applying an apical > basolateral gradient of [K] across the monolayer (20, 21). The passive movement of K through basolateral K channels (driven by the apical > basal gradient of [K]) elicited an I_{SC} (I_K) that was used to calculate basolateral P_K, as described below. The protocol was as follows: Apical NaCl Ringer's solution was replaced with a high K/low Na solution (no. 3, Table I), and basal NaCl Ringer's was replaced with low K/low Na solution (no. 4, Table I). Once I_{SC} transients had subsided (after 10 min), nystatin (0.022 mg/ml) was added to the apical solution to permeabilize this membrane. Cells were treated with 35 μM ouabain to inhibit the basolateral Na/K-ATPase and prevent its contributing to the I_K. These experiments were conducted in Cl-free solutions to prevent swelling-induced opening of K channels in the basal membranes of the cells (21). This allowed us to monitor the effects of carbachol and forskolin on the K channels in the absence of changes in cell volume. Similar results were obtained using Cl-containing solutions, though the magnitudes of the responses were larger by approximately 80%.

Apical Cl conductance was measured by permeabilizing the basolateral membrane with nystatin and then applying a basolateral > apical gradient of [Cl] across the monolayer. The passive movement of Cl through apical Cl channels (driven by the basal > apical gradient of Cl) elicited an I_{SC} (I_{Cl}) that was used to calculate apical P_{Cl}, as described below. NaCl Ringer's was changed to high Cl/high K (solution 5, Table I) on the basal side and Cl-free/high K (solution 6, Table I) on the apical side. Nystatin (0.022 mg/ml) was then added to the basolateral side to permeabilize this membrane.

Calculation of apical P_{Cl} and basolateral P_K from I_{Cl} and I_K measurements. Maximal current values for each condition (in μA/cm^2) were converted into fluxes (either I_K or I_{Cl}) by dividing by the Faraday constant F (96,500 coulombs/mol), and permeabilities were then calculated:

$$P_{Cl}\,(\text{cm/s}) = J_{Cl}\,(\text{mmol/cm}^2\cdot\text{s})/\Delta[\text{Cl}]\,(\text{mmol/cm}^3) \quad (1)$$

$$P_K\,(\text{cm/s}) = J_K\,(\text{mmol/cm}^2\cdot\text{s})/\Delta[\text{K}]\,(\text{mmol/cm}^3), \quad (2)$$

where Δ[Cl] and Δ[K] were equal to the differences between the ion concentrations on the apical and basolateral sides of the monolayer: 142 mM for the experiments on Cl and 135 mM for the experiments on K permeability, respectively.

Measuring P_{Cl} using SPQ. The Cl-sensitive dye SPQ was used to measure intracellular [Cl] (22). Cells were loaded with 10 mM SPQ,

added directly to the growth medium for 12–18 h at 37°C, similar to a procedure utilized previously (23). SPQ-loaded cells were mounted in a temperature-controlled (37°C) perfusion chamber on the stage of an inverted microscope (Zeiss IM35) for monitoring of fluorescence during rapid solution changes (2-s turnover, see reference 24). Intracellular (30–40 cells) SPQ was excited at 350 nm through a 40× Nikon Fluor (1.3 NA) objective emitted fluorescence (> 410 nm, one data point per second) was collected using a modular fluorimeter system (Fluorolog 2, model F2C, Spex Industries, Edison, NJ) attached to the inverted microscope. Fluorescence from SPQ-loaded cells was three to six times higher than the background signal recorded on unloaded cells.

Intracellular [Cl], Cl_i, was estimated from SPQ fluorescence using the double-ionophore calibration procedure described previously (22), with slight modification. At the end of an experiment the cells were perfused with calibration solutions containing 15 μM nigericin, 10 mM triphenyl-*N*-tin, 2.4 mM K_2HPO_4, 0.6 mM KH_2PO_4, 1 mM $MgSO_4$, 1 mM $CaSO_4$, 10 mM glucose, 10 mM Hepes, pH 7.4, and sequentially 135 mM KNO_3 and then 25 mM KCl-110 mM KNO_3, 50 mM KCl-85 mM KNO_3, and 135 mM KSCN. A calibration curve of F_o/F_x vs. [Cl] was constructed, where F_o was the difference in fuorescence signal obtained from cells bathed with KNO_3 Ringer's solution with [Cl] = 0 mM and from cells bathed with KSCN (to quench SPQ fluorescence); F_x was the difference in fluorescence measured at a given [Cl] and during KSCN perfusion.

To measure P_{Cl} induced by different agonists, cells were first perfused with NaCl Ringer's (no. 1, Table I) and then with $NaNO_3$ Ringer's (no. 2, Table I), which caused fluorescence to increase as Cl left the cell in a one-for-one exchange for NO_3 (Fig. 1). The rates of fluorescence increase were unaffected by 0.1 mM furosemide, which blocks $Na/K/Cl_2$ cotransport across the basolateral membranes of polarized cells, so measurements of SPQ fluorescence yield information about P_{Cl}. When fluorescence reached a plateau in $NaNO_3$ solution (due to the loss of cellular Cl), cells were perfused with nigericin+/triphenyl-*N*-tin-containing solutions with different [Cl], and fluorescence was converted to Cl_i by plotting F_o/F_x vs. [Cl] (Fig. 1). On

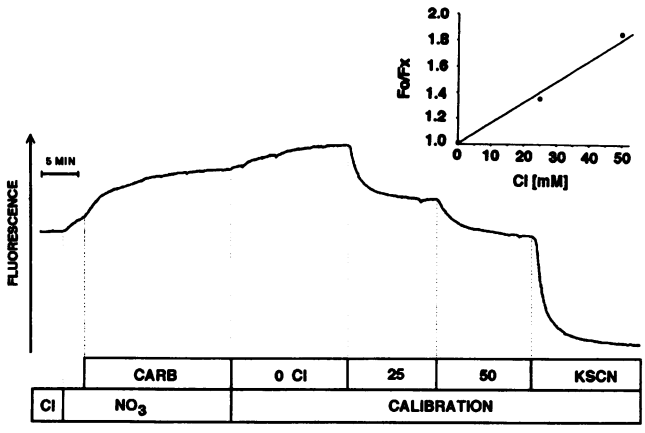

Figure 1. Measuring Cl_i and apical P_{Cl} with SPQ. Trace shows fluorescence of 30 T84 cells loaded with SPQ. Cells were bathed first with NaCl Ringer's (no. 1, Table I) and then with $NaNO_3$ (no. 2, Table I) as shown. This caused an increase in fluorescence as Cl left the cells in exchange for NO_3. Addition of 100 μM carbachol caused a further increase of fluorescence, indicating that carbachol induced an increase in P_{Cl}. The cells were then treated with calibration solution containing tributyl tin + nigericin and either 50, 25, or 0 mM Cl (substituted for NO_3; see Methods), and, at the end, KSCN solution to quench the SPQ fluorescence. The *Inset:* Calibration of the SPQ fluorescence in which the ratio of F_0 (difference between fluorescence in $NaNO_3$ and KSCN) to F_x (difference between fluorescence at of 0, 25, and 50 mM Cl and KSCN) was plotted vs. [Cl] to yield a calibration curve. This calibration is representative of six others.

average, resting cells had Cl_i = 53.6±4.4 mM (n = 6). Assuming an activity coefficient of 0.75, Cl activity in resting cells was 40.2 mM. This value agrees well with values of Cl_i, measured in a variety of epithelia using both SPQ (22) and ion-selective electrodes (25, 26).

The rates of change of Cl_i (mM/min) were converted into P_{Cl} using the following assumptions: (*a*) Cells were 10-μm cubes, with volume of 10^{-9} cm^3. (*b*) Surface area through which the flux occurred was 1/6 of the total surface area of the cell, i.e., 10^{-6} cm^2. (*c*) Buffering of Cl_i was nil. (*d*) NO_3-for-Cl exchange was one-for-one and therefore unaffected by the cell's membrane potential. (*e*) Cl_i under control conditions was 54 mM. Permeabilities were then calculated:

$$P_{Cl}\,(cm/s) = J_{Cl}\,(mmol/cm^2s)/\Delta[Cl]\,(mmol/cm^3) \quad (3)$$

Since calibration of Cl_i is a very time-consuming procedure, it was not performed in every experiment. For those experiments in which SPQ fluorescence was not calibrated, P_{Cl} was calculated as follows: the ratio of the rate of fluorescence increase just after agonist addition divided by the rate of fluorescence increase before agonist addition was determined. This ratio was then multiplied by the average value of P_{Cl} determined in resting cells from six independent calibrations (see Results).

Regulated exocytosis of Golgi-derived vesicles. T84 cells were grown on permeable polycarbonate membranes as for studies of I_{SC}. Development of $R_T > 800\ \Omega \cdot cm^2$ and an acidification of the basolateral medium (on average 0.3 pH units lower than pH of apical medium) were used as markers of tight junction formation. The labeling and quantitation of newly synthesized glycosaminoglycan (GAG) chains from Golgi-derived vesicles was performed using a slight modification of the assay described in detail by Miller and Moore (18). The assay is based on the following findigs: (*a*) Addition of a membrane-permeable xyloside, which serves as an acceptor for GAG chain elongation, induces synthesis of freely soluble GAG chains (27). (*b*) GAG chains become sulfated in the trans-Golgi apparatus (28, 29). Therefore, any GAG chains that have been secreted into the bathing media have come exclusively from vesicles derived from the Golgi apparatus during the time of incubation with xyloside and $^{35}SO_4$. These radiolabeled GAG chains can then be precipitated, filtered and quantitated (18, 30). This assay can be used reliably in T84 cells since xyoside inhibits synthesis of proteoglycans and thus during the 2-h labeling with $^{35}SO_4$ the cells do not incorporate radiolabel into other sulfated proteins (e.g., chondroitin sulfate proteoglycans; see below) in an amount which could complicate interpretation of the data.

Briefly, cells grown in six-well dishes on polycarbonate membranes (surface area = 4.5 cm^2) were first washed and then incubated at 37°C in a SO_4-free Ringer's saline (solution A) containing 110 mM NaCl, 5.4 mM KCl, 0.9 mM Na_2HPO_4, 10 mM $MgCl_2$, 2 mM $CaCl_2$, 1 g/liter glucose, 20 mM Hepes (pH 7.2), and 0.5 mM 4-methyl umbelliferyl-β-D-xyloside on both sides of the monolayers (500 μl on apical and 800 μl on basal side). After 30 min, this solution was aspirated and replaced with solution A containing 125 mCi/ml $^{35}SO_4$ (Amersham Corp., Arlington Heights, IL) and 0.5 mM xyloside for 2 h at 37°C to allow for accumulation of ^{35}S-labeled GAG chains in Golgi-derived vesicles.

After removal of the labeling medium, cells were washed quickly two times on both apical and basolateral sides with 1 ml of solution A supplemented with 4 mM Na_2SO_4 to stop labeling and remove unbound $^{35}SO_4$. The cells were then incubated at 37°C for two 1.5-h periods in serum-free DME H-21 medium to allow for release of GAG chains from the constitutive pathway. The solutions from both apical and basolateral surfaces were collected and stored for determination of the total amount of GAG secreted during the experiment. After a final rinse, serum-free DME H-21 medium containing either forskolin or carbachol was added to both sides of the cells, and these solutions were quickly collected and replaced with fresh aliquots at the time intervals indicated in the figures. All solutions and cells were maintained at 37°C during the entire procedure.

At the end of the collection periods, 100 μl of extraction buffer (solution B: 150 mM NaCl, 2 mM $MgCl_2$, 1% Triton X-100, and 50

mM Tris, pH 8.0), 100 μl of 6 mg/ml pronase E and 450 μl of PBS were added to both apical and basolateral sides, and the cells were digested over the course of 1 h at 37°C. This treatment allowed for the release of intracellularly stored or proteoglycan-attached GAG chains. Apical and basal media (500 and 800 μl total volume, respectively) containing $^{35}SO_4$-labeled GAG chains, secreted constitutively during the two 1.5-h chases or after stimultion, were also proteolytically digested during 1-h incubation at 37°C after adding 0.1 ml of 6 mg/ml pronase E.

GAG chains in the media and cell extracts were then precipitated (18, 30), by addition of 10% cetylpyridinium chloride (wt/vol, 2% final concentration) and 10 μl of 10 mg/ml chondroitin sulfate, during an additional 1-h incubation at 37°C. The samples were filtered through 0.45-μm Metricel GN-6 filters on a vacuum manifold and washed four times with 5 ml of 1% cetylpyridinium chloride 25 mM Na_2SO_4. The filters were dried and counted in a scintillation counter. Total radioactivity collected from both apical and basolateral media of each monolayer during the entre experiment was added to the radioactivity remaining in the cell extracts to yield "total GAG."

The results have been presented as (*a*) percentage of total GAG released or (*b*) "relative secretory rate." In this latter case, the percentage of total GAG released from carbachol- or forskolin-treated cells during a particular time interval (e.g., from 0 to 5 min or from 5 to 10 min, etc.) was divided by the percentage of total GAG released from control (untreated) cells during the same time interval. A minimum of two control and two experimental filters was used for each experiment.

Statistics. As indicated in the text, figures, and tables, data were often presented as means±SEM. Statistical significance was evaluated using a one-tailed *t* test, with $P < 0.05$ considered significant.

Results

Effects of carbachol and forskolin on I_{SC} (Cl transport) across intact monolayers. Both 100 μM carbachol and 10 μM forskolin caused similar increases of Cl secretion, but the time courses were different. Carbachol caused a rapid increase in I_{SC}, with a maximal response in 30 s, returning approximately to baseline within 2–5 min (Fig. 2 *A;* summary in Table II). Forskolin caused a slower, but more sustained, increase of I_{SC} (Fig. 2 *B;* Table II). Nearly identical ΔI_{SC} responses to forskolin were observed in monolayers that had been treated first with carbachol, and the I_{SC} response was allowed to decrease back to baseline before adding forskolin (not shown; experiments summarized in Table II). In contrast, when cells were treated first with forskolin and then with carbachol (Fig. 2 *B*), there was a much larger increase in I_{SC} as compared to the current resulting from treatment with carbachol alone (compare Fig. 2, *A* and *B;* see ΔI_{SC} values in Table II). It was also noted that, after the spikelike increase of Cl transport induced by carbachol, there was a small, delayed, but characteristic, increase in I_{SC} that usually was evident as a small "hump" in the current record 30–60 s after carbachol addition. This delayed effect of carbachol on the Cl transport will be discussed below.

Effects of carbachol and forskolin on I_{Cl} (apical Cl conductance) and I_K (basolateral K conductance) in nystatin-permeabilized monolayers. It is generally agreed for T84 cells that the cholinergic agonist carbachol causes basolateral K conductance to increase (2, 31, 32) owing to an increase in intracellular [Ca] (32), but the effects that carbachol and cell Ca exert in the regulation of apical Cl conductance is controversial (e.g., compare references 21, 23, and 33). Forskolin and other agents that raise cellular [cAMP] elicit large increases in apical P_{Cl} (21, 23, 33, 34), but the effects on basolateral P_K appear to be much smaller (35) or perhaps nonexistent (31). These disagreements may have arisen because some of the experiments have been performed on isolated cells, which may not have retained their normal polarity, while others have been performed on intact monolayers, which have tight junctions and distinct apical and basolateral membrane domains.

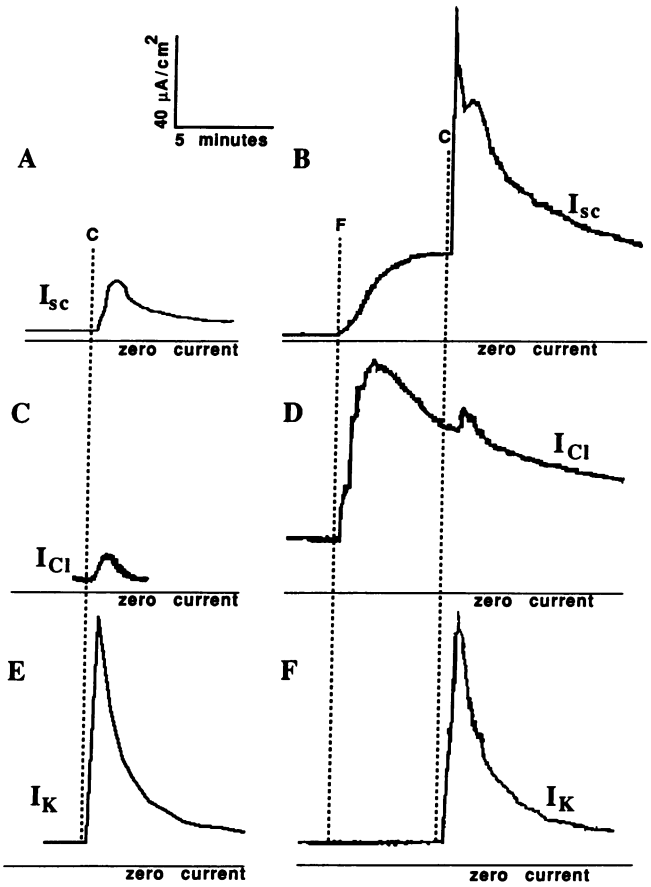

Figure 2. Time courses of effects of carbachol and forskolin on I_{SC} (net Cl secretion), I_{Cl}, and I_K across intact and permeabilized T84 monolayers. Stimulants were added as shown by the dotted lines, either 100 μM carbachol (*C*) alone or 100 μM forskolin (*F*) followed by carbachol. (*A* and *B*) Typical records showing the effects of the stimulants on I_{SC} (positive for Cl movement from basolateral to apical side) across intact monolayers with NaCl Ringer's on both sides of the epithelium. (*C* and *D*) I_{Cl} (positive for Cl movement from basolateral to apical side) of permeabilized monolayers which have high Cl/high K solution (no. 5, Table I) plus nystatin on the basal side and low Cl/high K solution (no. 6, Table I) on the apical side. (*E* and *F*) I_K (positive for K movement from apical to basal side) of permeabilized monolayers which have low K/low Na (no. 3, Table I) + ouabain on the basal side and high K/low Na solution (no. 4, Table I) plus nystatin on the apical side. Traces are representative of between 3 and 13 similar experiments.

To determine the effects of carbachol and forskolin on apical Cl conductance, cells were bathed on the apical side with a solution containing Cl-free/high K (solution 6, Table I) and on the basolateral side with high Cl/high K (solution 5) plus 0.022 mg/ml nystatin. There was a significant I_{Cl} ($\sim$ 32 μA/cm^2; see Table II) across permeabilized cells even before treatment with stimulants. Stimulation with carbachol caused a small, transient ($\approx$ 3 min) increase in I_{Cl} (Fig. 2 *C*), and the increase in I_{Cl} (ΔI_{Cl}) was approximately the same whether carbachol was added alone or followed forskolin treatment (Fig. 2 *D,* Table II). Forskolin caused a larger and more prolonged

Table II. I_{SC}, I_{Cl}, and I_K in Control, Untreated Monolayers and during Treatment with Stimulants

Treatment	I_{SC}	ΔI_{SC}	I_{Cl}	ΔI_{Cl}	I_K	ΔI_K
Control	3.6±2.8 (27)	—	31.8±8.2 (10)	—	10.2±2.5 (13)	—
Carbachol	22.6±5.3 (13)*	18.6±4.2 (13)[§]	58.8±23.3 (5)	29.8±9.8 (5)[a]	70.1±14.3 (13)*	59.9±12.3 (13)[a]
Forskolin	31.5±16.0 (14)*	28.6±16.0 (14)[§]	176.7±23.7 (5)*	142.0±15.8 (5)[a]	10.8±4.1 (7)	0 (7)
C + F	33.3±12.2 (8)	26.7±14.9 (8)[§]	122.9±22.0 (5)[#]	128.6±19.6 (5)[a]	36.2±13.9 (3)	0 (3)
F + C	93.6±29.2 (14)[‡]	70.3±25.1 (14)[§‖]	125.7±18.0 (5)	22.0±6.1 (5)[a]	71.4±13.1 (7)[#]	60.6±13.0 (7)[a]

Data represent maximum values measured during the different treatments. Differences Δ were obtained by subtracting the steady-state values before the treatment from the maximal values obtained during stimulation. C + F refers to cells that had been treated with carbachol and the transient responses were allowed to decrease back to low, steady-state values (after 5–10 min) before adding forskolin. F + C refers to cells which had been treated with forskolin for 5–10 min before adding carbachol. Numbers in parentheses represent the number of different monolayers. The following statistical comparisons were made: * $P < 0.05$ for I_{SC}, I_{Cl}, and I_K comparing control vs. carbachol or control vs. forskolin. [‡] $P < 0.05$ for I_{SC}, I_{Cl}, and I_K comparing carbachol + forskolin vs. carbachol and forskolin + carbachol vs. forskolin. [§] $P < 0.05$ for ΔI_{SC}, ΔI_{Cl}, and ΔI_K different from zero for carbachol, forskolin, carbachol + forskolin and forskolin + carbachol. [‖] $P < 0.05$ for ΔI_{SC}, ΔI_{Cl}, and ΔI_K comparing forskolin + carbachol vs. carbachol and carbachol + forskolin vs. forskolin.

increase in I_{Cl} (Fig. 2 *D*, Table II). When monolayers were treated first with carbachol and I_{Cl} was allowed to return to baseline, subsequent addition of forskolin exerted its typical effect, i.e., forskolin-induced ΔI_{Cl} was identical whether cells had been untreated or pretreated with carbachol (not shown; summarized in Table II). Thus, forskolin and carbachol both caused increases in I_{Cl}, and the responses (i.e., ΔI_{Cl}) were identical whether the stimulants were added alone or in combination.

To determine the K conductance of the basolateral membrane, cells were first bathed in Cl-free solutions containing high K (high K/low Na solution 3, Table I) plus nystatin on the apical side and low K (low K/low Na solution 4, Table I) plus 35 μM ouabain (to block the Na/K-ATPase) on the basolateral side. This created a gradient of [K] across the basolateral membrane of the permeabilized epithelium. Cl-free solutions were used to eliminate problems associated with KCl entry and cell swelling. When cells were stimulated with carbachol, I_K increased rapidly, but transiently. The carbachol-induced ΔI_K was the same when carbachol was added alone (Fig. 2 *E*) or followed stimulation with forskolin (Fig. 2 *F*). A summary of these experiments appears in Tables II and III. In contrast, forskolin had no effect on I_K (Fig. 2 *F*, Tables II and III). Also, when monolayers were treated first with carbachol and I_K was allowed to return to baseline, subsequent addition of forskolin had no effect on I_K (Tables II and III). Similar responses to the stimulants occurred in Cl-containing solutions, with the magnitudes of the responses ~ 80% larger than those observed in Cl-free solutions (not shown). Thus, carbachol, but not forskolin, increased I_K, and the ΔI_K response was the same whether carbachol was added to untreated cells or to cells pretreated with forskolin.

Table III. P_{Cl} and P_K: Resting, Carbachol, and Forskolin

Treatment	P_{Cl} (SPQ)	P_{Cl} (I_{Cl})	P_K (I_K)
		$\times 10^{-6}$ cm/s	
Control	2.1±1.0 (6)	2.4±0.6 (10)	0.8±0.3 (13)
Carbachol	6.2±2.6 (10)	4.4±1.7 (5)	5.2±1.1 (13)
Forskolin	23.0±6.2 (10)	13.1±1.8 (5)	0.8±0.3 (7)

Calculations were performed using data from Tables II and IV as described in Methods. P_{Cl} (SPQ) was calculated from rate of increase of SPQ fluorescence for control, untreated cells, and then during treatment with either carbachol or forskolin. P_{Cl} (I_{Cl}) and P_K (I_K) were calculated from magnitudes of I_{Cl} and I_K measured in untreated cells and then at the peak of the responses to carbachol or forskolin. Numbers in parentheses represent the number of different monolayers.

The time course of the increase in I_{SC} in response to forskolin corresponded well to the time course of the increase of I_{Cl} (compare Fig. 2, *B* and *D*). When carbachol was then added to these forskolin-treated cells to induce the synergistic effect, there was an increase in I_{SC} that occurred simultaneously with the increase in I_K (compare Figs. 2 *B* and *F*). After the carbachol-induced spike in I_{SC} and I_K, there was a small, delayed increase ("hump") in I_{Cl} that correlated well with the activation of a small, but detectable, increase in apical Cl conductance.

Effects of carbachol and forskolin on P_{Cl} measured with SPQ. Rapid changes in P_{Cl} in response to carbachol and forskolin were measured using the protocol shown in Fig. 3 (summarized in Tables III and IV). This approach avoids the permeabilization procedures utilized in the electrophysiological experiments and thereby provides a good control. Carbachol (Fig. 3 *A*) caused P_{Cl} to increase by about 3-fold, and forskolin (Fig. 3 *B*) caused P_{Cl} to increase on average by > 11-fold. As shown in Fig. 3 *C*, when cells were treated first with carbachol, P_{Cl} often appeared to increase only transiently (for 2–3 min), and subsequent addition of forskolin to these cells caused a subsequent, rapid increase of SPQ fluorescence, similar to that elicited by forskolin alone. When cells were treated first with forskolin, addition of carbachol had no further effect (not shown). This was likely because during forskolin treatment in $NaNO_3$-Ringer's, SPQ fluorescence increased from the control to the maximum level (i.e., equal to that in zero Cl) in about 7 s, and, since our assay required the presence of some Cl in the cell, further measurements of P_{Cl} could not be performed. However, when forskolin and carbachol were added simultaneously, the increase in P_{Cl} was the same as adding forskolin alone.

Quantitation of Golgi-to-plasma membrane traffic using GAG as tracer. The magnitudes and time courses of exocytosis of Golgi-derived vesicles with the apical and basolateral plasma membranes were compared with the time courses and magnitudes of the carbachol- and forskolin-stimulated changes in I_{SC},

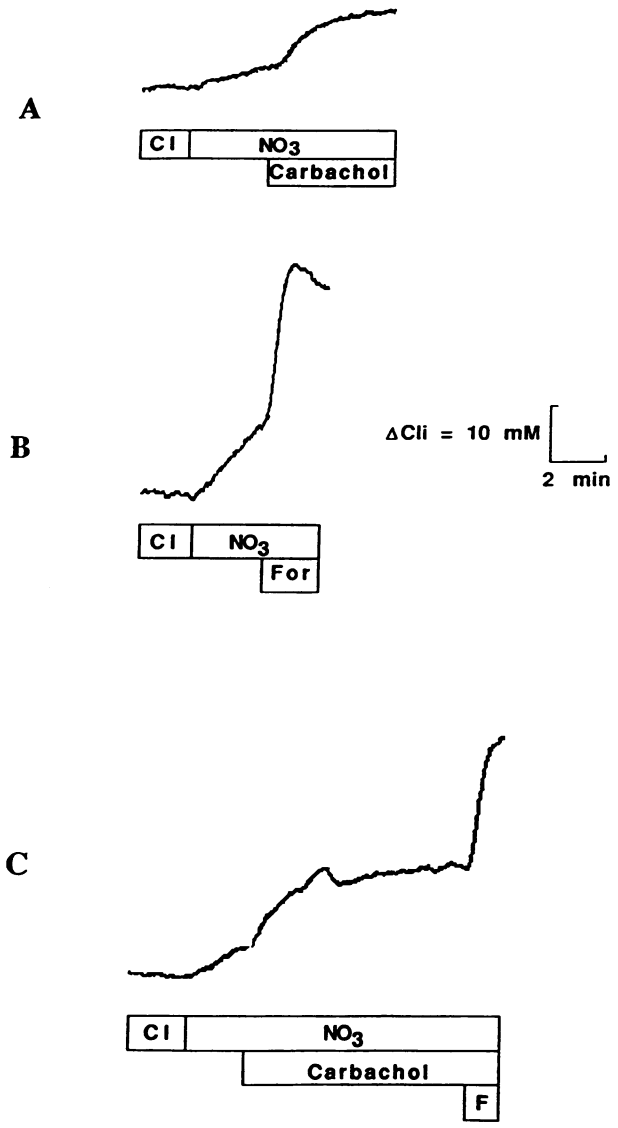

Figure 3. Effects of carbachol and forskolin on P_{Cl} as measured with SPQ. P_{Cl} was measured by exchanging NaCl Ringer's (no. 1, Table I) with $NaNO_3$ Ringer's (no. 2, Table I) and measuring the rate of increase of SPQ fluorescence (i.e., decrease of Cl_i). (*A*) Carbachol caused the rate of Cl_i loss to increase from 1.6 to 10.0 mM/min. (*B*) Forskolin caused Cl_i loss to increase from 7.4 to 61.9 mM/min. (*C*) Addition of carbachol and then forskolin elicited the characteristic responses of each stimulant. Carbachol caused P_{Cl} to increase from 3.8 to 15.0 mM/min and this effect seemed to be transient because the increased rate of loss of Cl reached a plateau after about 2 min of carbachol treatment. Subsequent treatment with forskolin caused P_{Cl} to increase to 48.9 mM/min.

P_K, and P_{Cl}. If there were stimulant-induced increases in apical and basolateral exocytosis that correlated with the changes of apical P_{Cl} and basolateral P_K, then it raises the possibility that ionic permeabilities are regulated at least in part by the exocytotic insertion of vesicles containing channels into the apical and basolateral membranes.

To confirm that T84 cells can be induced to synthesize GAG chains by xyloside, cells grown on permeable supports were first starved for 30 min in SO_4-free medium containing 0, 2, 5, and 10 mM xyloside and then radiolabeled for 2 h with

Table IV. P_{Cl} Measured with SPQ

Treatment	Rate of Cl loss	*n*
	mM/min	
Control	5.1±0.6	6
Carbachol	14.9±2.0*	10
Forskolin	56.4±4.7*	10
Carbachol + forskolin	59.5±9.1‡	3

SPQ-labeled T84 monolayers were perfused first with NaCl Ringer's (no. 1, Table I), and fluorescence was measured in 30–40 cells. Under these conditions, Cl_i averaged 54 mM (see Methods). NaCl Ringer's was switched to $NaNO_3$ Ringer's (no. 2, Table I) to measure P_{Cl} under resting (Control) conditions, and then after adding carbachol or forskolin or forskolin on top of carbachol. Statistical comparisons: * $P < 0.05$ for comparisons carbachol vs. control and forskolin vs. control. ‡ $P < 0.05$ for comparison carbachol + forskolin vs. carbachol.

166 μCi/ml of $^{35}SO_4$ at 37°C in the presence of the same concentrations of xyloside as during starvation. The cells were then chased in unlabeled media for 1 h, apical and basolateral media were collected, and secreted macromolecules were precipitated with acetone at −20°C, separated on 12.5% polyacrylamide gel and autoradiographed (Fig. 4). In the absence of xyloside there was a negligible amount of $^{35}SO_4$-labeled GAG chains secreted into either apical or basolateral side of the cell. The presence of xyloside induced synthesis of free GAG chains, as can be judged from the characteristic molecular weight distribution (18, 30). A fraction of these newly synthesized GAG chains were secreted into both apical and basolateral solutions. During further tests, 0.5 and 2.0 mM xyloside were found to elicit nearly equivalent GAG chain production, and 0.5 mM xyloside was used in all subsequent experiments. Notice that very little labeled high molecular weight specific species were secreted using the $^{35}SO_4$-labeling protocol.

Various cultured intestinal cells are able to synthesize and secrete mucins (36–38), including T84 cells (39). McCool et al. (39) showed that T84 cells release 0.5–0.7% of the total cell mucus in 30 min, and stimulation by 1 mM carbachol increased this to 2%. Thus, some mucin secretion is expected from the apical surface during our 2-h collection. According to McCool et al. (39) these mucins have very high molecular weight and do not enter 7.5% separating gels. As shown in Fig. 4, the amount of $^{35}SO_4$-labeled high molecular weight material was negligible; i.e., there was only a small amount of $^{35}SO_4$-labeled high molecular weight material that did not enter the 12.5% separating gels, indicating that very little labeled mucin was released as compared to GAG. It is likely that the apparently small mucin secretion is due to xyloside-induced synthesis (and release) of GAG chains, and concomitant inhibition of proteoglycan synthesis (30).

Fig. 5 *A* shows the typical pattern of secretion of the GAG chains expressed as the percentage of the total label secreted from untreated cells and in response to 100 μM carbachol during 30 min. More than twofold greater secretion was directed toward the basolateral than toward the apical surface of both carbachol-treated and control cells, and carbachol caused increased rates of GAG secretion into both the apical and basolateral solutions (i.e., compared to the untreated controls). The

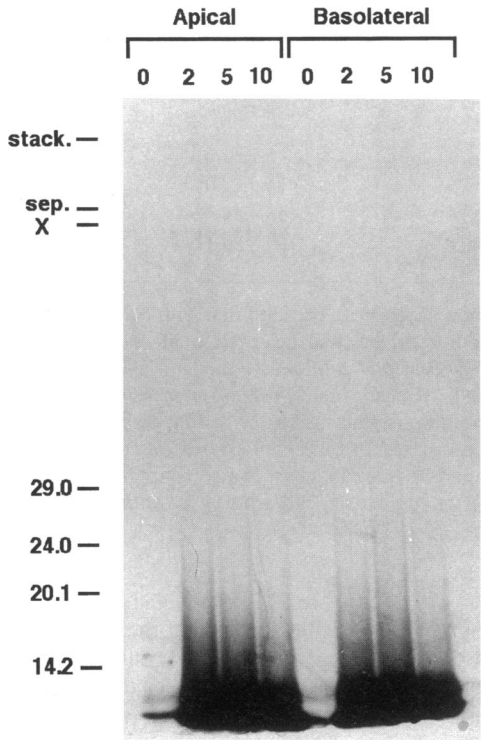

Figure 4. Induction of synthesis and secretion of GAG chains by xyloside. The cells were labeled with $^{35}SO_4$ for 2 h in the presence of 0, 2, 5, and 10 mM xyloside. Apical and basolateral media were then collected, GAG chains precipitated, separated on 12.5% polyacrylamide gel, and autoradiographed. The beginning of stacking and separating gels are marked "stack." and "sep.," respectively. A longer exposure of this gel revealed the presence of a high molecular weight material (marked *X*) below the top of the 12.5% separating gel. This material is probably not mucin because it enters the 12.5% gel (39). The smeared species migrating around 14.2 kD are xyloside-GAG chains, which were much more abundant than the high molecular weight species (*X*).

effect of carbachol on the relative rates of GAG secretion toward the apical and basal solutions at different times after stimulation are shown in Fig. 5 *B*. In this case, the amount of GAG secreted during the different time intervals (0–2, 2–5, 5–10, 10–15, and 15–30 min) in the carbachol treated cells were divided by the values obtained for the same time periods from untreated controls. Plotting the data in this way emphasizes the effects of carbachol on the relative rate (i.e., compared to the untreated controls) of GAG secretion into the apical and basal solutions during the time intervals shown. It should be remembered, though, that the amount of GAG secreted into the basal solution was always larger than that secreted into the apical solution. As shown in Fig. 5 *B*, carbachol induced a rapid (i.e., occurring during the 0–2-min time interval) increase in the rate of GAG secretion to the apical and basolateral solutions; the relative increase was larger at the apical side than at the basal side; the effect of carbachol was more prolonged at the basolateral than at the apical side. Eight experiments monitoring carbachol-dependent GAG secretion are shown in Fig. 6, *A* and *B*. Carbachol did not increase the relative rate of GAG chain release when the agonist was added to the apical side, indicating that the response was receptor-specific (acetylcholine receptors are located only on the basolateral sides in these polarized cells). Note that the rate of exocytosis to both apical and basal solutions increased during the first minute following carbachol addition.

Forskolin also increased GAG secretion, but the pattern was distinctly different from that induced by carbachol. Forskolin caused a somewhat delayed (i.e., it was not evident until 5 min) increase in the rate of secretion directed mainly toward the apical surface (Fig. 7 *A*), and secretion toward the basolateral surface was essentially unaffected by forskolin (Fig. 7 *B*).

Results of experiments with cross-stimulation are shown in Figs. 8 and 9. In carbachol-treated cells, forskolin did not alter the relative rate of GAG secretion toward either the apical (Fig. 8 *A*) or basolateral (Fig. 8 *B*) sides. In forskolin-treated cells, carbachol increased GAG chain secretion to the apical solution

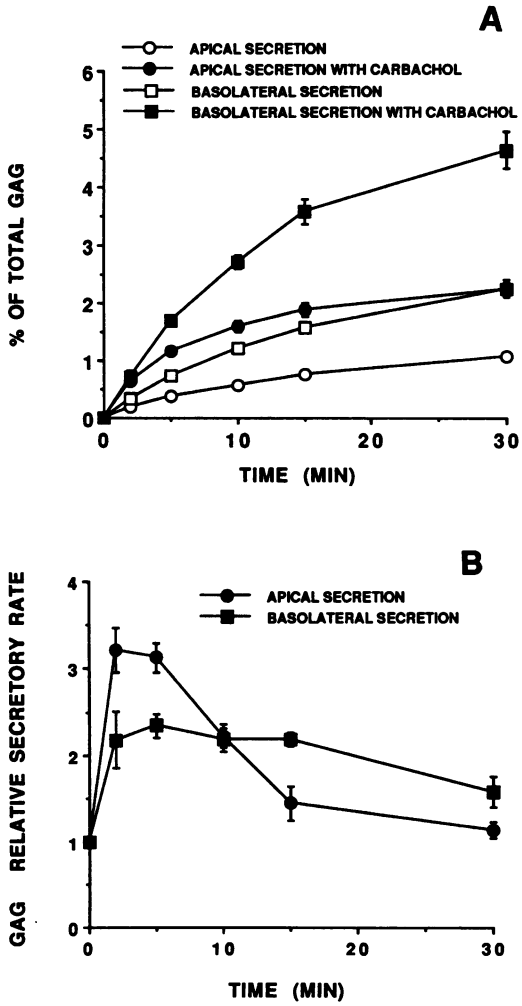

Figure 5. Secretion of $^{35}SO_4$-labeled GAG chains into the apical and basal solutions of T84 monolayers during treatment with carbachol. (*A*) Time course of release of GAG chains expressed as a percentage of the total amount of GAG $^{35}SO_4$-labeled into the apical and basal solutions in control (i.e., untreated) and carbachol-treated (beginning at $t = 0$) monolayers. (*B*) Relative rate (compared to the untreated, resting monolayers) of secretion of GAG to the apical and basolateral solutions during treatment with carbachol (beginning at $t = 0$) for the time periods 0–2, 2–5, 5–10, 10–15, and 15–30 min. These graphs are based on the results from one experiment. The error bars show SEM for three replicates of each time point. In the cases where there are no error bars shown, SEM were smaller than the symbols.

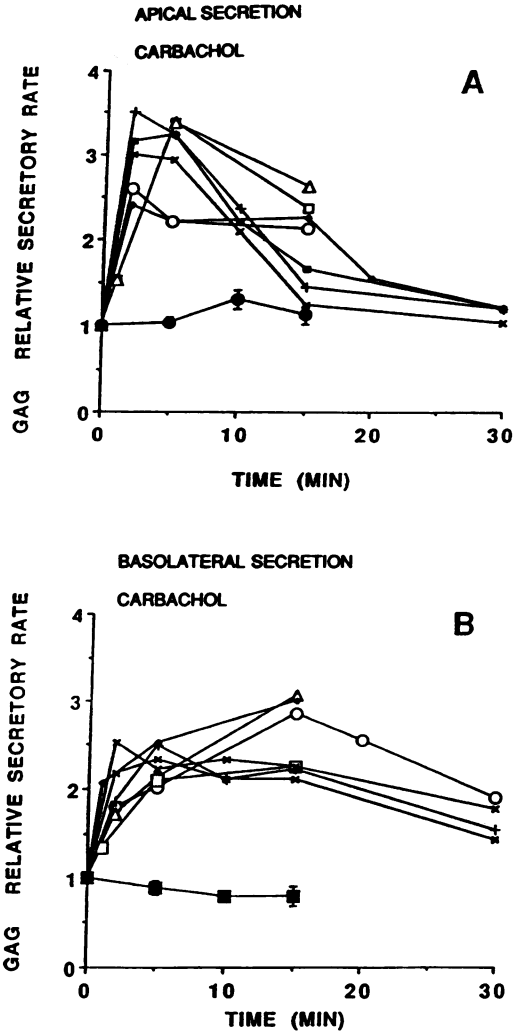

Figure 6. Effects of carbachol on relative rates of secretion of GAG chains into the (*A*) apical and (*B*) basolateral solutions. Summary of data showing the effects of adding (at time 0) carbachol to either the apical (closed circles or squares) or basolateral (all other symbols) bathing solution. Data are expressed relative to untreated controls for the time intervals shown (0–1 or 0–2, 2–5, etc.). The error bars on the closed circles show SEM for different experiments in which carbachol was added to the apical solution.

(Fig. 9 *A*) and also toward the basolateral side (Fig. 9 *B*) with time courses and magnitudes that were similar to those induced by carbachol alone (Fig. 6).

Discussion

Effects of carbachol and forskolin on Cl transport, apical P_{Cl}, and basolateral P_K. Carbachol caused a rapid, but transient, increase in Cl transport primarily, though not exclusively (see below), through a similarly timed 6.5-fold increase in basolateral P_K. The carbachol-induced activation of these basolateral K channels (2, 21, 31, 32, 34) appears to be due to the increases of intracellular [Ca] (21, 23, 32, 40). Carbachol also induced a small (1.8–2.9 fold), and somewhat delayed, increase in apical P_{Cl}. These results are in agreement with Lindeman and Chase (23), who found an 84% increase in apical P_{Cl} with ionomycin (which also raises intracellular [Ca]). Others have similarly found evidence for the presence of Ca-activated Cl channels (33, 35), but the apical vs. basolateral location of these channels was not determined. In contrast, Anderson and Welsh (20) found that treatment of T84 cells with Ca ionophore (which also raises intracellular [Ca]) did not increase apical P_{Cl}. As noted previously (21), these different results may be due to different strains of T84 cells, or to other subtleties associated with culturing techniques. Whether the effects noted here are on CFTR or on another Cl channel remains to be determined.

Forskolin caused large (5.5–11-fold) and, compared to carbachol's effects, relatively sustained effects on apical P_{Cl}. This stimulatory effect of forskolin on P_{Cl} has been observed previously (20, 22, 33–35, 41), but the quantitation and polarity of the effect is provided for the first time here. There were no effects of forskolin on basolateral P_K. It has been previously concluded that cAMP either activates (42) or has no effect (33) on basolateral P_K. Our data with permeabilized cells (in which the apical or basolateral membrane is voltage-clamped to 0

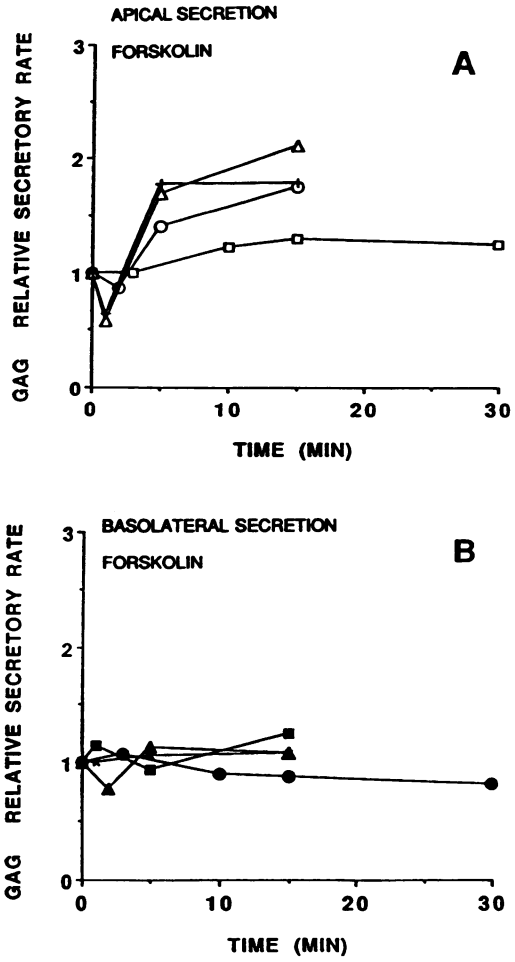

Figure 7. Effects of forskolin on relative rates of GAG chain secretion into the (*A*) apical and (*B*) basal solutions. Summary of data from four different monolayers showing the effects of adding (at time 0) forskolin to the basal side of intact monolayers bathed with NaCl Ringer's on both sides. Data are expressed relative to untreated controls for the time intervals shown (0–1, 1–5, etc.). There was a delayed, but characteristic, increase of GAG chain secretion to the apical solution. There were no effects of forskolin on GAG chain secretion to the basal side.

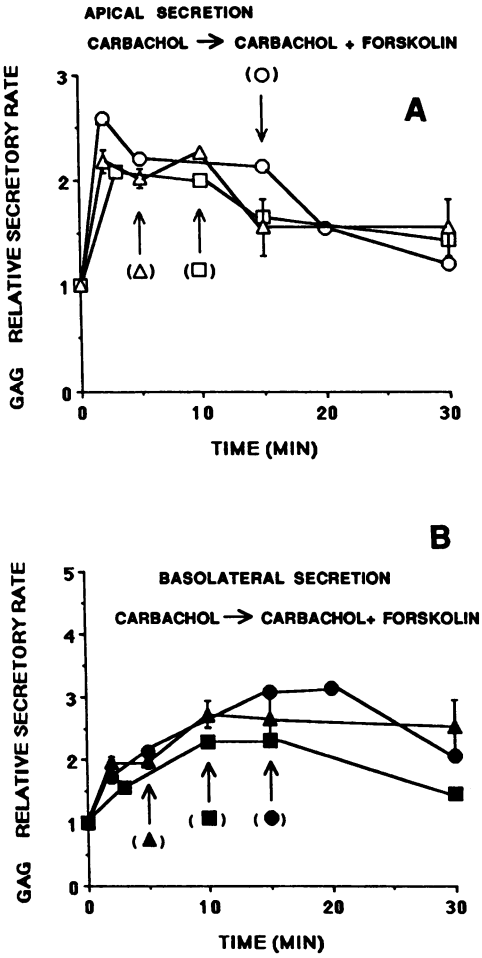

Figure 8. Effects of adding carbachol and then forskolin on relative rate of GAG chain secretion into the (*A*) apical and (*B*) basal solutions. Summary of data from three monolayers showing the effect of adding carbachol (at time 0) and then forskolin after 5, 10, or 15 min of stimulation with carbachol (as shown by arrows). Data are expressed relative to untreated controls for time intervals shown. Carbachol caused the characteristic increase in GAG chain secretion to both the apical and basal solutions, and forskolin had no further effect on the relative rate of GAG chain secretion. The error bars show SEM for three replicates of each time point. In the cases where there are no error bars shown, SEM were smaller than the symbols.

mV) indicate that, in intact cells, the apparent stimulatory effects of cAMP on P_K were due to increases of apical P_{Cl}, which caused changes of membrane potential and indirect effects on K fluxes, although there may also be cell culture conditions that can account for these differences.

Carbachol increases Cl secretion across the apical membrane primarily because P_K increases, which causes cellular membrane voltage (V_{cell}) to hyperpolarize, thereby increasing the driving force for Cl to leave the cell. The increase in Cl secretion will not reach maximal levels, though, because apical P_{Cl} is activated only to a relatively small extent. Forskolin, which increases P_{Cl} to very high levels, also causes relatively small increases in Cl secretion and this results from the fact that basolateral P_K remains low, and V_{cell} is likely too small to drive Cl out of the cell at a maximal rate. Since carbachol and forskolin exert their characteristic effects on P_K and/or P_{Cl} whether added alone or in combination with the other agonist (as shown by the equal responses of ΔI_K and ΔI_{Cl}—see Table II), synergism between carbachol and forskolin in the stimulation of Cl secretion is not due to the combined effects of the stimulants to activate the apical Cl or basolateral K channels to a greater degree than with either stimulant alone. Instead, synergism occurs when the stimulants are added in such a way that the apical Cl and the basolateral K channels are activated synchronously, i.e., timing of the addition of forskolin and carbachol is critical. When cells are treated with forskolin first, cellular [cAMP] and apical P_{Cl} remain elevated for an extended time. When carbachol is then added, basolateral P_K and V_{cell} both increase while apical P_{Cl} is still elevated, thereby eliciting

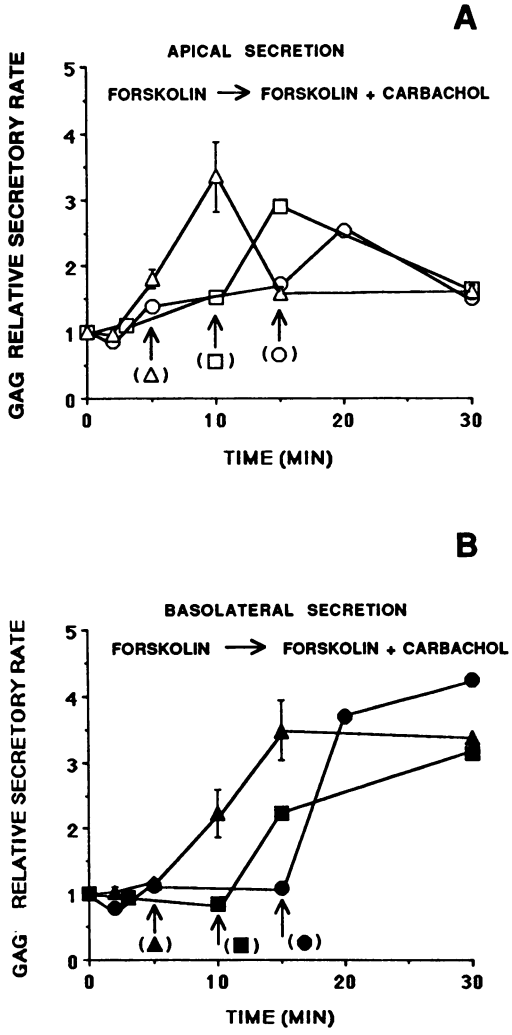

Figure 9. Effects of adding forskolin and then carbachol on relative rate of GAG chain secretion into the (*A*) apical and (*B*) basal solutions. Summary of data from three different monolayers showing the effects of adding forskolin (at time 0) and then carbachol at 5, 10, and 15 min, as shown by arrows. Data are expressed relative to untreated controls for time intervals shown. Note that forskolin caused small increases of GAG chain secretion to the apical side but no effect on secretion to the basal side. Subsequent addition of carbachol to the forskolin-treated monolayers caused larger increases in GAG secretion to both sides of the monolayers that approximated those occurring during addition of carbachol alone. The error bars show SEM for three replicates of each time point. In the cases where there are no error bars shown, SEM were smaller than the symbols.

maximal Cl secretion. In contrast, when carbachol is added first, its large stimulation of basolateral P_K and V_{cell} (and small effect on apical P_{Cl}) dissipates rapidly. When forskolin is added after the carbachol effect has subsided back to baseline, P_{Cl} increases, but Cl secretion will remain small because P_K and V_{cell} are small.

Are P_{Cl} and P_K regulated by exocytosis of Golgi-derived vesicles with the apical and basolateral membranes? Exocytosis is a common mechanism for the rapid secretion of macromolecules by various cell types. Some epithelial cells also secrete abundant amounts of stored proteins, which can be labeled and detected after secretion, thereby serving as an excellent measure of regulated exocytosis (43). In addition, many recent reports have stressed the importance of agonist-stimulated exocytosis for the function of epithelial cells that secrete ions (4, 5, 7–9, 13, 14). Although T84 cells do not have easily identifiable secretory markers, the sulfated GAG utilized here can serve as an ideal fluid-phase marker for all vesicles derived from the trans-Golgi complex to quantitate exocytosis of newly synthesized, Golgi-derived vesicles to both apical and basolateral sides. This assay can be used reliably in T84 cells because there is little $^{35}SO_4$ incorporation into either mucins (Fig. 4) or other secreted sulfated proteins (not shown) during the two hour labeling period used for our experiments.

In the resting state there was a substantial baseline rate of secretion of the GAG chains to both the apical and basolateral solutions. This constitutive secretion of GAG likely reflects normal membrane turnover (i.e., constitutive exocytosis) at the two sides of the cells. The twofold larger secretion to the basal side than to the apical side may partially reflect the larger surface area at the basal and lateral sides of the cells. Because the volume of the cells remains constant during this time, the constitutive rate of exocytosis at both apical and basal surfaces must be balanced by equal rates of endocytosis at both membranes. Bradbury and colleagues (13, 14) have shown using the uptake of horseradish peroxidase that T84 cells do indeed exhibit a constitutive rate of fluid phase endocytosis, and it will be important to determine whether this was occurring at the apical and/or basolateral sides of the cells.

Carbachol caused a rapid, transient, two- to threefold increase of GAG release to the apical solution and a more sustained two- to threefold increase in release to the basal solution. During the 30 min after stimulation, only 6–9% of total labeled intracellular GAG chains was secreted. Because T84 cells secrete mucins in response to carbachol (39), it is possible that the carbachol-induced increases in GAG secretion to the apical surface is related to mucus secretion. However, this possibility is not very likely for the following reasons: First, the time course of carbachol-stimulated GAG secretion to the apical surface did not correlate with that reported for mucin secretion. Marcon et al. (37) and McCool et al. (39) found that carbachol induced mucin secretion was linear for at least 30 min, while we found GAG secretion to be maximal within 2–5 min after addition of carbachol and declining sharply during the next 10 min, reaching the basal unstimulated levels by 30–60 min (Figs. 5 and 6 *A*). Second, mucin secretion only occurs apically, whereas carbachol characteristically stimulated GAG releases to both apical and basolateral surfaces. The relatively low rates of GAG secretion may be due to the fact that mechanisms regulating exocytosis are not as well developed in culture as compared with in vivo. Another possibility is that there is a relatively small amount of vesicular traffic associated with ion secretion.

The time course of these effects of carbachol on rates of exocytosis were similar to the effects of carbachol on ion permeability and transport; i.e., all effects were observed during the first minute after carbachol addition. Although we cannot determine whether the carbachol-induced increases in apical and basolateral GAG secretion precede or follow the increases in P_{Cl} and P_K, the data indicate that these events may be related to each other. Thus, it seems possible that the carbachol-induced increases in P_K and P_{Cl} are elicited, at least in part, by the fusion of cytoplasmic vesicles with the apical and basolateral plasma membranes. Such exocytotic events could also be important for secretagogue-stimulated delivery of other transporters (e.g., $NaKCl_2$ cotransport and Na/K-ATPase) to the basolateral surfaces of the cells. In support of this hypothesis, preliminary experiments have shown that nocodazole (causes microtubule breakdown) inhibited forskolin and carbachol-stimulated GAG secretion and I_{SC}, both by ~ 60% (data not shown).

Forskolin also caused small increases in the delivery of GAG chains to the apical, but not to the basal, side. Although we cannot determine whether there is a causal relationship between the cAMP-activated delivery of Golgi-derived vesicles and the activation of apical Cl channels, because forskolin caused increases in P_{Cl} and GAG secretion at the apical side of the cell and there were no changes of P_K or GAG secretion at the basolateral side, there may be a relationship between exocytosis and activation of membrane channels during forskolin treatment too. However, the small forskolin-induced increases in GAG secretion coupled with recent experiments showing that the amount of CFTR at the apical membrane does not change during cAMP stimulation (16) indicate that exocytosis is likely not the major mechanism for regulating apical P_{Cl} during cAMP stimulation in T84 cells.

It should also be noted that there was no simple correlation between exocytosis and activation of membrane K and Cl channels. Carbachol caused 1.8–2.9-fold increases in P_{Cl} and 2–3-fold increases in apical GAG secretion, while forskolin caused 5.5–11-fold increases of P_{Cl} but only 1.5–2.0-fold increases in apical GAG secretion; after carbachol treatment, forskolin had its typically large effect on P_{Cl} but no effect on apical exocytosis; and carbachol elicited transient increases in P_K but more prolonged increases in exocytosis to the basolateral membrane. Thus, our data suggest that ion permeability in T84 cells may be regulated both by exocytosis and also by direct activation through second messengers (e.g., Ca, protein kinases, phosphorylation, etc.). However, further experiments will be necessary to dissect the relative contribution of each pathway. The GAG secretion assay for quantitating polarized exocytosis should provide a valuable tool for such studies.

Acknowledgments

We thank Hoon Kang, Athe Tsibris, and Thilo Weisflog for help with some of the experiments to determine basolateral K conductance; Beate Illek, Aldebaran Hofer and Horst Fischer for reading and commenting on the manuscript; and Amy Robinson for tireless editorial and secretarial assistance.

This work was supported by grants from the National Institutes of Health (DK19520 to TEM and GM35239 to H-PHM), the Cystic Fibrosis Foundation (Z441 to Dr. Machen), and Cystic Fibrosis Research, Inc. (M1720 to Dr. Machen).

References

1. Dharmsathaphorn, K., K. G. Mandel, H. Masui, and J. A. McRoberts. 1985. Vasoactive intestinal polypeptide-induced chloride secretion by a colonic epithelial cell line: direct participation of a basolaterally localized Na^+, K^+, Cl^- cotransport system. *J. Clin. Invest.* 75:462–471.

2. Dharmsathaphorn, K., and S. Pandol. 1986. Mechanism of chloride secretion by carbachol in a colonic epithelial cell line. *J. Clin. Invest.* 77:348–354.

3. Welsh, M. J. 1986. The Respiratory Epithelium: Physiology of Membrane Disorders. T. E. Andreoli, J. F. Hoffman, D. D. Fanestil, and S. G. Schultz, editors. Plenum Publishing Corp., New York.

4. Forte, T., T. E. Machen, and J. G. Forte. 1977. Ultrastructural changes in oxyntic cells associated with secretory function: a membrane recycling hypothesis. *Gastroenterology.* 73:941–955.

5. Gluck, S., C. Cannon, and Q. Al-Awqati. 1982. Exocytosis regulates urinary acidification in turtle bladder by rapid insertion of H^+ ATPase into the luminal membrane. *Proc. Natl. Acad. Sci. USA.* 79:4327–4331.

6. Brown, D., S. Hirsch, and S. Gluck. 1988. An H^+-ATPase in opposite plasma membrane domains in kidney epithelial cell subpopulations. *Nature (Lond.).* 331:622–4.

7. Brown, D. 1989. Vesicle recycling and cell-specific function in kidney epithelial cells. *Ann. Rev. Physiol.* 51:771–784.

8. Bae, H.-R., and A. S. Verkman. 1990. Protein kinase A regulated chloride conductance in endocytic vesicles from proximal tubule. *Nature (Lond.).* 348:637–639.

9. Bacskai, B. J., and P. A. Friedman. 1990. Activation of latent Ca^{2+} channels in renal epithelial cells by parathyroid hormone. *Nature (Lond.).* 347:388–291.

10. Yiu, S. C., R. W. Lambert, M. E. Bradley, C. E. Ingham, K. L. Hales, R. L. Wood, and A. K. Mircheff. 1988. Stimulation-associated redistribution of Na, K-ATPase in rat lacrimal gland. *J. Membr. Biol.* 102:185–194.

11. Yiu, S. C., R. W. Lambert, P. J. Tortoriella, and A. K. Mircheff. 1991. Secretagogue-induced redistribution of Na, K-ATPase in rat lacrimal acini. *Invest. Ophthalmol. Visual Sci.* 32:2976–2984.

12. Buanes, T., T. Grotmol, T. Landsverk, and M. G. Raeder. 1987. Ultrastructure of pancreatic duct cells at secretory rest and during secretin-dependent $NaHCO_3$ secretion. *Acta Physiol. Scand.* 131:55–62.

13. Bradbury, N. A., T. Jilling, G. Berta, E. J. Sorscher, R. J. Bridges, and K. L. Kirk. 1992. Regulation of plasma membrane recycling by CFTR. *Science (Wash. DC).* 256:530–532.

14. Bradbury, N. A., T. Jilling, K. L. Kirk, and R. J. Bridges. 1992. Regulated endocytosis in a chloride secretory epithelial cell line. *Am. J. Physiol.* 262(Cell Physiol. 31):C752–C759.

15. Prince, L., A. Tousson, and R. B. Marchase. 1993. Cell surface labeling of CFTR in T84 cell. *Am. J. Physiol.* 264:C491–C498.

16. Denning, G. M., L. S. Ostedgaard, S. H. Cheng, A. E. Smith, and M. J. Welsh. 1992. Localization of cystic fibrosis transmembrane conductance regulator in chloride secretory epithelia. *J. Clin. Invest.* 89:339–349.

17. Dharmsathaphorn, K., J. A. McRoberts, K. G. Mandel, L. D. Tisdale, and H. Masui. 1984. A human colonic tumor cell line that maintains vectorial electrolyte transport. *Am. J. Physiol.* 246(Gastrointest. Liver Physiol. 9):G204–G208.

18. Miller, S. G., and H. P. Moore. 1992. Movement from the trans-Golgi network to cell surface in semi-intact cells. *Methods Enzymol.* 219:234–248.

19. Lewis, S. A., D. C. Eaton, C. Clausen, and J. M. Diamond. 1977. Nystatin as a probe for investigating the electrical properties of a tight epithelium. *J. Gen. Physiol.* 70:427–440.

20. Anderson, M. P., and M. J. Welsh. 1991. Calcium and cAMP activate different chloride channels in the apical membrane of normal and cystic fibrosis epithelia. *Proc. Natl. Acad. Sci. USA.* 88:6003–6007.

21. Wong, S. M. E., A. Tesfaye, M. C. DeBelly, and H. S. Chase. 1990. Carbachol increases basolateral K conductance in T-84 cells. *J. Gen. Physiol.* 96:1271–1285.

22. Chao, A. C., J. H. Widdicombe, and A. S. Verkman. 1990. Chloride conductive and cotransport mechanism in cultures of canine tracheal epithelial cells measured by an entrapped fluorescent indicator. *J. Membr. Biol.* 113:193–202.

23. Lindeman, R. P., and H. S. Chase. 1992. Protein kinase C does not participate in carbachol's secretory action in T84 cells. *Am. J. Physiol.* 263:C140–C146.

24. Negulescu, P. A., and T. E. Machen. 1990. Intracellular ion activities and membrane transport in parietal cells measured with fluorescent probes. *Methods Enzymol.* 192:38–81.

25. Shorofsky, S. R., M. Field, and H. A. Fozzard. 1984. Mechanism of Cl secretion of canine trachea: changes in intracellular chloride activity with secretion. *J. Membr. Biol.* 81:1–8.

26. Smith, J. J., J. D. McCann, and M. J. Welsh. 1990. Bradykinin stimulates airway epithelial Cl^- secretion via two second messenger pathways. *Am. J. Physiol.* 258:L369–L377.

27. Schwartz, N. B., L. Galigani, P.-L. Ho, and A. Dorfman. 1974. Stimulation of synthesis of free chondroitin sulfate chains by β-D-xylosides in cultured cells. *Proc. Natl. Acad. Sci. USA.* 71:4047–4051.

28. Kimura, J. H., S. Lohmander, and V. C. Hascall. 1984. Studies on the biosynthesis of cartilage proteoglycan in a model system of cultured chondrocytes from the Swarm rat chondrosarcoma. *J. Cell Biochem.* 26:261–278.

29. Velasco, A., J. Hidalgo, J. Perez-Villar, G. Garcia-Herduge, and P. Navas. 1988. Detection of glycosaminoglycans in the Golgi complex of chondrocytes. *Eur. J. Cell Biol.* 47:241–250.

30. Luikart, S. D., J. L. Sackrison, and C. V. Thomas. 1985. Altered glycosaminoglycan production by HL-60 cells treated with 4-methylumbelliferyl-β-D-xyloside. *Blood.* 66:866–872.

31. Devor, D. C., S. M. Simaski, and M. E. Duffy. 1990. Carbachol induces oscillations of membrane potassium conductances in a colonic cell line, T84. *Am. J. Physiol.* 256:C318–C326.

32. Wong, S. M. E., R. P. Lindeman, S. Parangi, and H. S. Chase. 1989. Role of calcium in mediating action of carbachol T84 cells. *Am. J. Physiol.* 257:C976–C985.

33. Cliff, W., and R. A. Frizzell. 1990. Separate Cl^- conductances activated by cAMP and Ca^{2+} and Cl^- secreting epithelial cells. *Proc. Natl. Acad. Sci. USA.* 87:4956–4960.

34. Cartwright, C. A., J. A. McRoberts, K. G. Mandel, and K. Dharmsathaphorn. 1985. Synergistic action of cyclic adenosine monophosphate- and calcium-mediated chloride secretion in a colonic epithelial cell line. *J. Clin. Invest.* 76:1837–1842.

35. Venglarik, C. J., R. J. Bridges, and R. A. Frizzell. 1990. A simple assay for agonist-regulated Cl and K conductances in salt-secreting epithelial cells. *Am. J. Physiol.* 259(Cell Physiol. 28):C358–C364.

36. Phillips, T. E., C. Muet, P. R. Bilbo, D. K. Podolsky, D. Louvard, and M. R. Neutra. 1988. Human intestinal goblet cells in monolayer culture. Characterization of a mucus-secreting subclone derived from the HT29 colonic adenocarcinoma cell line. *Gastroenterology.* 94:1390–1403.

37. Marcon, M. A., D. McCool, J. Forstner, and G. Forstner. 1990. Inhibition of mucin secretion in a colonic adenocarcinoma cell line by DIDS and potassium channel blockers. *Biochim. Biophys. Acta.* 1052:17–23.

38. Forstner, G., Y. Zhang, D. McCool, and J. Forstner. 1993. Mucin secretion by T84 cells: stimulation of PCK, Ca^{2+}, and protein kinase activated by Ca^{2+} ionophore. *Am. J. Physiol.* 264:G1096–G1102.

39. McCool, D. J., M. A. Marcon, J. F. Forstner, and G. G. Forstner. 1990. The T-84 human colonic adenocarcinoma cell line produces mucin in culture and releases it in response to various secretagogues. *Biochem. J.* 267:491–500.

40. Reinlib, L., R. Mikkelson, D. Zahniger, K. Dharmsathophorn, and D. Donowitz. 1989. Carbachol-induced cytosolic free Ca^{2+} increases in T84 colonic cells seen by microflourimetry. *Am. J. Physiol.* 257:G950–G960.

41. Mandel, K. G., K. Dharmsathophorn, and J. A. McRoberts. 1986. Characterization of a cyclic AMP-activated Cl^- transport pathway in the apical membrane of a human colonic epithelial cell line. *J. Biol. Chem.* 261:704–712.

42. Mandel, K. G., J. A. McRoberts, G. Buerlein, E. S. Foster, and K. Dharmsathaphorn. 1986. Ba^{2+} inhibition of VIP and A23187 stimulated Cl-secretion by T-84 cell monolayers. *Am. J. Physiol.* 250(Cell Physiol. 19):C486–C494.

43. Paul, A., M. Mergey, D. Veissiere, B. Hermelin, G. Cherqui, J. Picard, and C. B. Basbaum. 1991. Regulation of secretion in cultured tracheal serous cells by protein kinases A and C. *Am. J. Physiol.* 261:L172–L177.